ORIGINAL ARTICLE

Respective Effects of Helmet Pressure Support, Continuous Positive Airway Pressure, and Nasal High-Flow in Hypoxemic Respiratory Failure
A Randomized Crossover Clinical Trial

Luca S. Menga[1,2*], Luca Delle Cese[1,2*], Tommaso Rosà[1,2], Melania Cesarano[1,2], Roberta Scarascia[1,2], Teresa Michi[1,2], Daniele G. Biasucci[1,2], Ersilia Ruggiero[1,2], Antonio M. Dell'Anna[1,2], Salvatore L. Cutuli[1,2], Eloisa S. Tanzarella[1,2], Gabriele Pintaudi[1,2], Gennaro De Pascale[1,2], Claudio Sandroni[1,2], Salvatore Maurizio Maggiore[3,4], Domenico L. Grieco[1,2], and Massimo Antonelli[1,2]

[1]Department of Emergency, Intensive Care Medicine and Anesthesia, Fondazione Policlinico Universitario A. Gemelli IRCCS, Rome, Italy; [2]Istituto di Anestesiologia e Rianimazione, Università Cattolica del Sacro Cuore Rome, Italy; [3]University Department of Innovative Technologies in Medicine and Dentistry, Gabriele d'Annunzio University of Chieti-Pescara, Chieti, Italy; and [4]Department of Anesthesiology, Critical Care Medicine and Emergency, SS. Annunziata Hospital, Chieti, Italy

ORCID IDs: 0000-0002-1828-9143 (S.M.M.); 0000-0002-4557-6308 (D.L.G.).

Abstract

Rationale: The respective effects of positive end-expiratory pressure (PEEP) and pressure support delivered through the helmet interface in patients with hypoxemia need to be better understood.

Objectives: To assess the respective effects of helmet pressure support (noninvasive ventilation [NIV]) and continuous positive airway pressure (CPAP) compared with high-flow nasal oxygen (HFNO) on effort to breathe, lung inflation, and gas exchange in patients with hypoxemia ($Pa_{O_2}/F_{I_{O_2}} \leqslant 200$).

Methods: Fifteen patients underwent 1-hour phases (constant $F_{I_{O_2}}$) of HFNO (60 L/min), helmet NIV (PEEP = 14 cm H_2O, pressure support = 12 cm H_2O), and CPAP (PEEP = 14 cm H_2O) in randomized sequence.

Measurements and Main Results: Inspiratory esophageal (ΔP_{ES}) and transpulmonary pressure (ΔP_L) swings were used as surrogates for inspiratory effort and lung distension, respectively. Tidal Volume (V_T) and end-expiratory lung volume were assessed with electrical impedance tomography. ΔP_{ES} was lower during NIV versus CPAP and HFNO (median [interquartile range], 5 [3–9] cm

H_2O vs. 13 [10–19] cm H_2O vs. 10 [8–13] cm H_2O; $P = 0.001$ and $P = 0.01$). ΔP_L was not statistically different between treatments. $Pa_{O_2}/F_{I_{O_2}}$ ratio was significantly higher during NIV and CPAP versus HFNO (166 [136–215] and 175 [158–281] vs. 120 [107–149]; $P = 0.002$ and $P = 0.001$). NIV and CPAP similarly increased V_T versus HFNO (mean change, 70% [95% confidence interval (CI), 17–122%], $P = 0.02$; 93% [95% CI, 30–155%], $P = 0.002$) and end-expiratory lung volume (mean change, 198% [95% CI, 67–330%], $P = 0.001$; 263% [95% CI, 121–407%], $P = 0.001$), mostly due to increased aeration/ventilation in dorsal lung regions. During HFNO, 14 of 15 patients had pendelluft involving >10% of V_T; pendelluft was mitigated by CPAP and further by NIV.

Conclusions: Compared with HFNO, helmet NIV, but not CPAP, reduced ΔP_{ES}. CPAP and NIV similarly increased oxygenation, end-expiratory lung volume, and V_T, without affecting ΔP_L. NIV, and to a lesser extent CPAP, mitigated pendelluft.

Clinical trial registered with clinicaltrials.gov (NCT04241861).

Keywords: noninvasive ventilation; acute hypoxemic respiratory failure; helmet support; acute respiratory distress syndrome

The optimal noninvasive management of acute hypoxemic respiratory failure is debated. High-flow nasal oxygen (HFNO) is the currently suggested first-line intervention (1, 2). Face mask noninvasive ventilation (NIV) is also widely used to treat these

patients (3). However, several concerns exist regarding the use of this technique because of the risk of self-inflicted lung injury and the detrimental effect of delayed intubation on the clinical outcome of patients who fail NIV (4). In recent years, there has been renewed

interest in NIV deployed via the helmet interface (5–7). Compared with face masks, helmets enable longer-term treatments with good patient comfort (8) and permit the use of higher positive end-expiratory pressure (PEEP) (9, 10). In spontaneously breathing

patients with hypoxemic respiratory failure, high PEEP improves oxygenation and may mitigate the risk of self-inflicted lung injury (11–13).

A preliminary randomized trial showed lower rates of intubation and mortality in patients with acute respiratory distress syndrome treated with continuous positive airway pressure (CPAP) or NIV delivered through the helmet interface compared with a face mask (14). Helmet support has also been used to treat coronavirus disease (COVID-19) respiratory failure, with promising but conflicting results (15–17). However, few data are available to discriminate the physiological effects of high PEEP delivered during helmet NIV and CPAP in patients with hypoxemia, and these two techniques are often applied interchangeably in clinical practice.

We conducted a crossover randomized study to assess the respective effects of high-PEEP helmet NIV and CPAP compared with HFNO on effort to breathe, respiratory mechanics, gas exchange, and lung inflation during moderate-to-severe hypoxemic respiratory failure.

Some of the results of this study have been previously reported in the form of an abstract (18).

Methods

This is the primary report of a randomized crossover clinical trial (clinicaltrials.gov: NCT04241861) conducted in the ICU of a university hospital in Italy between January 2020 and January 2021. The local ethics committee (ID 2693) approved the study, and all patients provided written informed consent before study entry.

Patients
Adult patients admitted to the ICU with acute respiratory failure were assessed for enrollment. Patients were considered

eligible if all the following inclusion criteria were met (19):

1. $Pa_{O_2}/F_{I_{O_2}} \leq 200$ was measured in the supine position after 15 minutes of treatment with the nonrebreather face mask connected to the high-flow system (60 L/min; temperature of the humidification chamber set at 37°C; $F_{I_{O_2}}$, 50%). Given the use of high flows, nominal $F_{I_{O_2}}$ was considered a reliable estimate of the actual $F_{I_{O_2}}$.
2. $Pa_{CO_2} < 45$ mm Hg.
3. No history of chronic respiratory failure or moderate to severe cardiac insufficiency (New York Heart Association class greater than II or left ventricular ejection fraction < 50%).

Exclusion criteria:

*   Exacerbation of asthma or chronic obstructive pulmonary disease;
*   Cardiogenic pulmonary edema;
*   Hemodynamic instability (systolic blood pressure < 90 mm Hg or mean arterial pressure < 65 mm Hg) and/or lactic acidosis (lactate > 5 mmol/L) and/or clinical signs of shock;
*   Metabolic acidosis (pH < 7.30 with normal or hypocarbia);
*   Glasgow Coma Scale score < 13;
*   Recent head surgery or anatomy preventing the use of a helmet or HFNO on the patient's face.

Protocol
Enrolled patients received the three interventions in a randomized crossover manner for 1 hour each. Between study phases, to avoid any carry-over effect, a 20-minute period of Venturi mask oxygen therapy was delivered. If an $F_{I_{O_2}} > 60\%$ was needed, a nonrebreather face mask connected to the high-flow system was applied.

Interventions
HFNO. HFNO was delivered with the AIRVO2 device (Fisher and Paykel Health Care). The flow was set at 60 L/min, and the humidification chamber was heated at 37°C, 34°C, or 31°C, according to the patient's comfort (20).

Helmet NIV. We used NIV-dedicated helmets (Dimar SRL). The size was chosen according to neck circumference (8). Patients were connected to a gas-based ventilator through a bitube circuit with no humidification (21).

The ventilator was set in pressure support mode as follows (22, 23):

*   Pressure support = 10–12 cm H_2O;ROI
*   PEEP = 14 cm H_2O;
*   inspiratory flow trigger = 2 L/min;
*   fastest pressurization time;
*   expiratory trigger: 30% of the maximum inspiratory flow;
*   maximum inspiratory time: 1.2 seconds.

Helmet CPAP. We used CPAP-dedicated helmets (Dimar SRL), the size of which was chosen according to neck circumference (8). Treatment was delivered through an air–oxygen blender connected to the patient through a single-limb circuit and a PEEP valve. We applied the following settings: *1)* continuous airflow 60 L/min (21, 24); *2)* PEEP 14 cm H_2O. The pressure inside the helmet was confirmed by an external manometer.

With all interfaces, $F_{I_{O_2}}$ was adjusted to obtain an oxygen saturation as measured by pulse oximetry (Sp_{O_2}) ≥ 92% and ≤98% in the initial 15 minutes of the study phase. Sedatives/opioids were not administered in any study phase.

Measurements
Patient demographics and clinical characteristics were collected at study entry.

During the study, patients underwent standard monitoring, including heart rate,

Correspondence and requests for reprints should be addressed to Domenico L. Grieco, M.D., Department of Emergency, Intensive Care Medicine and Anesthesia, Fondazione Policlinico Universitario A. Gemelli IRCCS, Rome, 2 Italy. E-mail: dlgrieco@outlook.it.

This article has a related editorial.

This article has an online supplement, which is accessible from this issue's table of contents at www.atsjournals.org.

At a Glance Commentary

Scientific Knowledge on the Subject: The use of the helmet interface in patients with acute hypoxemic failure is increasing worldwide. Helmets can be used in either continuous positive airway pressure (CPAP) or pressure support noninvasive ventilation (NIV) mode. The respective effects of positive end-expiratory pressure with and without pressure support (NIV and CPAP, respectively) delivered through the helmet interface on effort to breathe, gas exchange, and lung inflation need to be better understood.

What This Study Adds to the Field: In this randomized crossover study, we assessed the physiological effects of helmet CPAP and NIV in patients with moderate-to-severe hypoxemic respiratory failure ($Pa_{O_2}/F_{I_{O_2}} \leq 200$) compared with high-flow nasal oxygen, which is considered the standard of care for these patients. Compared with high-flow nasal oxygen, helmet NIV, but not CPAP, decreased inspiratory effort, measured through esophageal manometry. Neither NIV nor CPAP significantly affected lung distension assessed by inspiratory transpulmonary pressure swings. Helmet NIV and CPAP similarly improved blood oxygenation, mostly because of increased recruitment of the dorsal regions of the lung, as assessed by electrical impedance tomography. Both CPAP and NIV increased V_T (measured as tidal impedance variation) but reduced lung dynamic strain. In our population of nonintubated patients with hypoxemia, the pendelluft phenomenon was common and was mitigated by helmet support, especially when applied with NIV. Helmet NIV and CPAP have different physiological effects, especially regarding their impact on inspiratory effort. Helmet NIV could be helpful in patients exhibiting intense inspiratory effort before treatment initiation, whereas helmet CPAP could be preferred if the inspiratory effort is low.

invasive blood pressure, and Sp_{O_2}. A polyfunctional nasogastric tube provided with an esophageal balloon (Nutrivent, Sidam) was placed and secured at a depth of 38–42 cm to measure esophageal pressure (P_{ES}). The esophageal balloon was filled with 4 ml of air, which is a nonstress volume ensuring reliability within a wide pressure range for the Nutrivent (25–27). To ensure intraindividual reproducibility, the esophageal balloon was deflated and, after checking adequate zeroing, reinflated before all measurements. An electrical impedance tomography belt (LuMon, Sentec) with 16 electrodes was placed around the thorax between the fifth or sixth parasternal intercostal space and connected to a dedicated device to record electrical impedance signals. To ensure intrapatient reproducibility, the patients lay in the semirecumbent position, with a bed inclination of 45°, throughout all study phases. Impedance data were acquired at a frame rate of 40 Hz.

Electrical impedance tomography measurements are usually expressed in arbitrary units that quantify the amplitude of impedance changes within pixels (28). However, it is difficult to relate arbitrary units to clinical data; hence, assuming that impedance changes are proportional to changes in volume, we present impedance-related results throughout the text as volume percentage change compared with HFNO; the absolute impedance values (arbitrary units) are displayed in Table 2.

A full description of impedance signal processing is detailed in the online supplement.

A pressure transducer measured P_{ES}, and, during helmet NIV and CPAP, a pneumotachograph placed at the end of the inspiratory limb of the circuit measured inspiratory flow and airway pressure.

At the end of each phase, the following data were collected:

- Respiratory rate, Sp_{O_2}, pH, Pa_{CO_2}, Pa_{O_2}, Sa_{O_2}, $Pa_{O_2}/F_{I_{O_2}}$;
- Heart rate and arterial blood pressure;
- Dyspnea and discomfort, as defined by a visual analog scale (VAS) adapted for ICU patients (29–32) (see Figures E1 and E2 in the online supplement);
- Fifteen-minute impedance signal;
- Fifteen-minute P_{ES} and, during CPAP and NIV, airway pressure and flow signals.

Airway pressure, flow, P_{ES}, and electrical impedance tomography signals were acquired in phase, amplified, low-pass filtered, digitalized at 40 Hz, and stored in a personal computer (Fluxmed, MBMED). All breaths from the last 15 minutes of each study phase were analyzed with MATLAB (Mathworks). The results from all breaths in the 15-minute recording were averaged for each study step.

Endpoints
The primary aim of the study was to assess the effects of helmet NIV and helmet CPAP, compared with HFNO, on inspiratory effort (i.e., ΔP_{ES}) and V_T, defined as the amount of gas inflating the lungs during the breath cycle as measured with electrical impedance tomography (Figure 1 and online supplement) (33).

The secondary endpoints of the study were as follows:

1. Breathing pattern: respiratory rate, VAS dyspnea and discomfort, P_{ES} pressure–time product per minute (online supplement), and quasistatic transpulmonary pressure (ΔP_L), defined as the difference between end-inspiratory transpulmonary pressure and end-expiratory transpulmonary pressure. The chest wall recoil pressure for the calculation of P_{ES} pressure–time product per minute was derived from the measured lung compliance, assuming a constant chest wall–to–respiratory system elastance ratio of 0.27 (34).
2. Gas exchange.
3. Lung volumes and inflation pattern: V_T size and distribution in the four regions of interest (ROIs) of the lung (ventral, midventral, middorsal, dorsal; ROIs were defined from a standardized lung contour per patient and are specific for the impedance software used [Figure E3]); amount of pendelluft, expressed in terms of percentage V_T and calculated as described in the online supplement (33, 36, 37); end-expiratory lung impedance (EELI), derived from the impedance signal and the lung strain definition (35, 38, 39) (online supplement); regional EELI in the four ROIs (online supplement); and dynamic lung strain, computed as the ratio of V_T to the FRC. For this purpose, FRC was approximated to EELI during HFNO, whereas in helmet
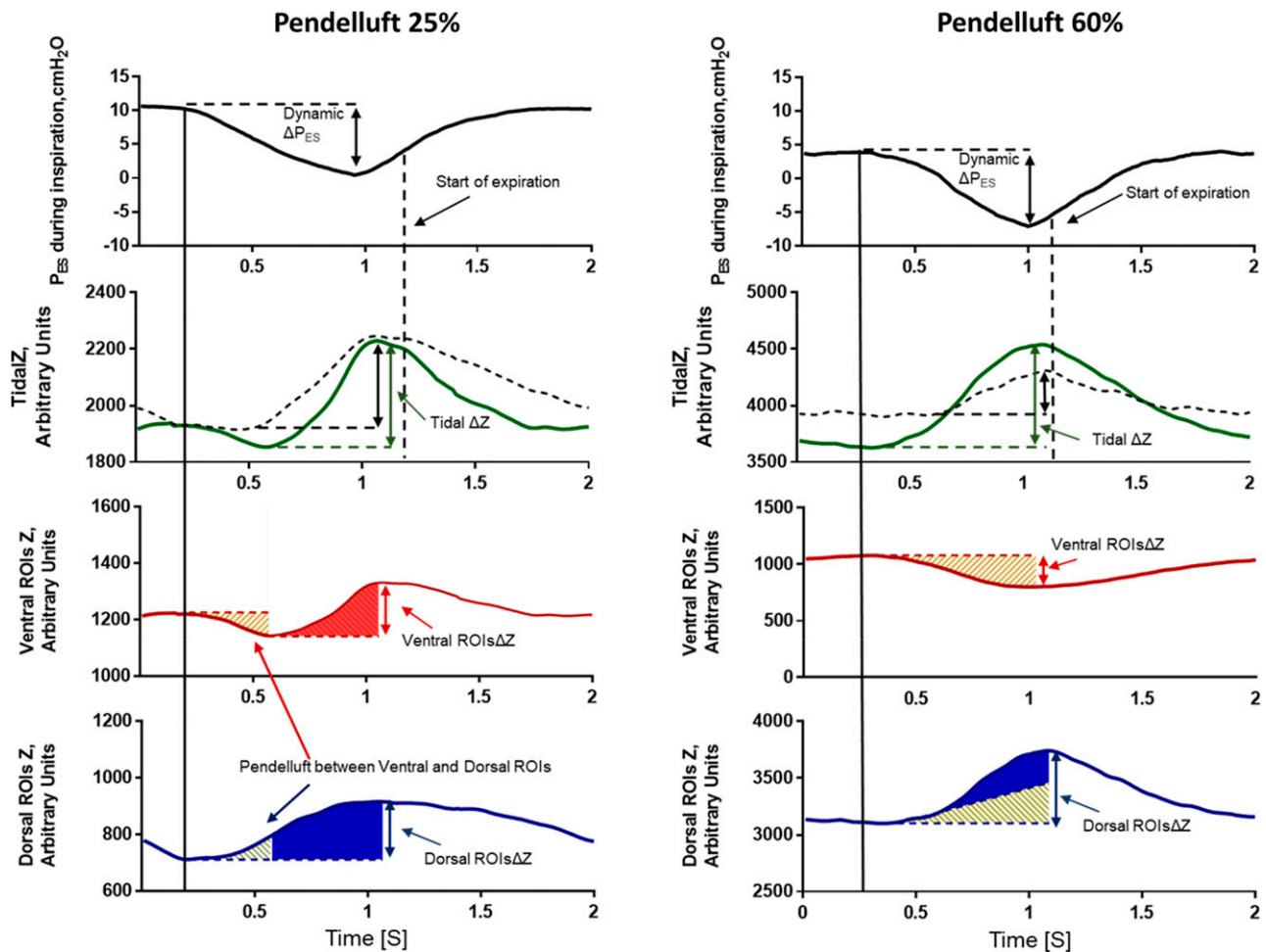
Figure 1. Representative figure of two patients (left and right panels) during the trial, showing pendelluft between the ventral and dorsal regions of the lung. Pendelluft percentage was calculated as described in the Methods and the online supplement. In both patients, during muscular inspiration (first panel), air moves from the ventral regions of interest (ROIs) (third panel) toward the dorsal ROIs (fourth panel) and vice versa during muscular expiration. This pendelluft effect is represented as the yellow area that moves from the ventral ROIs (third panel) to the dorsal ROIs (fourth panel). The second panel shows tidal impedance variation (TidalΔZ, a surrogate of V_T) computed as: *1*) the difference between the end-expiratory and end-inspiratory impedance during the breathing cycle (dashed line); and *2*) the gas inflating the lungs during the breathing cycle, calculated on a pixel-by-pixel basis (solid green line). TidalΔZ, computed as the difference between the end-expiratory and end-inspiratory impedance (dashed line), does not consider the intratidal shift between the ventral and dorsal ROIs. This yields underestimation of the volume of lung distension, especially in the dorsal regions. TidalΔZ, calculated on a pixel-by-pixel basis (solid green line), represents a more accurate estimate of the amount of lung distension. A detailed description of the TidalΔZ calculation is provided in the online supplement. P_{ES} = esophageal pressure; ROIsΔZ = tidal impedance variation within ROIs; ΔP_{ES} = inspiratory effort.

steps, we considered as recruited volume the difference in EELI in the dorsal regions between helmet phases and the HFNO phase (online supplement) (39, 40); regional dynamic strain, computed as above, for the four ROIs; the amount of overstretched lung regions, defined as the percentage of pixels on the lung impedance map with a dynamic strain greater than two (39). Consistent with a previous investigation (27), airway pressure was assumed to be constant and equal to 2.5 cm H_2O for all calculations in

the HFNO step (27, 41). For all calculations, the end of inspiration was defined based on the impedance versus time curve when its first derivative became negative (Figure 1).

Sample Size Calculation
Given the physiological design of the study, we did not perform a formal sample size calculation. Consistent with previous investigations on the topic (27, 42), we planned to enroll a convenience sample of 15 patients.

Statistical Analysis
Categorical data are expressed as the event rate (%), and continuous data are expressed as the median (interquartile range). For repeated measures, ordinal qualitative variables or quantitative variables in the three study steps were compared with ANOVA for repeated measures, with Bonferroni's correction added for paired comparisons. If the assumption of sphericity was violated, we used the Friedman test with Dunn's correction for paired comparisons. *P* values, mean differences, and confidence intervals (CIs) for paired comparisons were adjusted for multiple

comparisons (Bonferroni's or Dunn's, as appropriate), and results with $P \le 0.05$ were considered statistically significant.

Correlations between continuous variables were assessed with Pearson's correlation, and the r and P values are reported. All analyses were performed by applying a bilateral hypothesis. Statistical analysis was performed with SPSS 26.0, MATLAB R2021, and GraphPad Prism V 7.00.

Results

The demographics and clinical characteristics of the enrolled patients are shown in Table 1. The median (interquartile range) $Pa_{O_2}/F_{I_{O_2}}$ at enrollment was 120 (103–137) mm Hg, and the median Pa_{CO_2} was 34 (27–37) mm Hg, with the most hypoxemic patients being the most hypocapnic ($r = 0.63$; $P = 0.01$) (Figure E4).

Data on VAS dyspnea and VAS discomfort were missing in one patient, but there were no other missing data.

Effort to Breathe and Respiratory Mechanics
These results are displayed in Table 2.

Compared with HFNO, helmet NIV, but not helmet CPAP, reduced ΔP_{ES} (mean difference, −5 cm H_2O [95% CI, −8 to −1 cm H_2O]; $P = 0.01$ and 3 cm H_2O [95% CI, 7 to −1 cm H_2O]; $P = 0.17$, respectively;

Figure 2). ΔP_L and respiratory rate did not differ between treatments (Figures 2 and 3).

Compared with HFNO, P_{ES} pressure–time product per minute did not change with helmet CPAP and NIV ($P = 0.34$, $P = 0.56$). However, the P_{ES} pressure–time product during helmet NIV was lower than that during CPAP (mean difference, −146 cm $H_2O \cdot sec \cdot min^{-1}$ [95% CI, −235 to −59 cm $H_2O \cdot sec \cdot min^{-1}$]; $P = 0.002$) (Figure 2).

Compared with HFNO, VAS discomfort was higher during helmet CPAP ($P = 0.008$) but not during helmet NIV ($P = 0.11$) (Figure 3). VAS dyspnea was not significantly different between treatments (all $P > 0.05$).

Determinants of Respiratory Effort
ΔP_{ES} was proportional to the degree of hypocapnia and hypoxemia during CPAP and HFNO but not during helmet NIV (Figure E5).

The reduction in ΔP_{ES} produced by NIV was greater among patients exhibiting the most intense ΔP_{ES} while on HFNO and helmet CPAP; consequently, patients with low ΔP_{ES} during HFNO and CPAP experienced increases in ΔP_L when submitted to helmet NIV (Figure E6).

Gas Exchange
These results are displayed in Table 2.

Compared with HFNO, helmet CPAP and helmet NIV significantly improved

$Pa_{O_2}/F_{I_{O_2}}$ (Figure 3), with a mean difference of 78 mm Hg (95% CI, 39–117 mm Hg; $P = 0.001$) and 50 mm Hg (95% CI, 20–81 mm Hg; $P = 0.002$), respectively; $Pa_{O_2}/F_{I_{O_2}}$ was not different between CPAP and NIV ($P = 0.13$).

Pa_{CO_2} was not different between treatments (all $P > 0.05$).

Tidal Volume
These results are displayed in Table 3.

Compared with HFNO, V_T increased with helmet CPAP and NIV (mean percentage change, 93% [95% CI, 30–155%], $P = 0.002$; 70% [95% CI, 17–122%], $P = 0.02$, respectively), with no significant difference between NIV and CPAP ($P = 0.32$) (Figure 4). The increase in V_T was prominent in the dorsal regions of the lung.

Pendelluft was detected with all interfaces. Pendelluft involving >10% of V_T was observed in 14/15 patients during HFNO, 12/15 patients during helmet CPAP, and 10/15 patients during helmet NIV. The amount of pendelluft, expressed as percentage of V_T, was inversely related to $Pa_{O_2}/F_{I_{O_2}}$ ($r = 0.58$; $P < 0.001$) and was proportional to the ratio $\Delta P_{ES}/PEEP$ ($r = 0.35$; $P = 0.02$) (Figure E8).

Compared with HFNO, pendelluft decreased significantly with helmet CPAP (mean difference, −17% [95% CI, −31 to −3%]; $P = 0.01$) and further with helmet NIV (mean difference, −23% [95% CI, −39 to −8%]; $P = 0.004$) (Figures 4 and 5).

EELI
These results are displayed in Table 3.

Compared with HFNO, helmet NIV and CPAP increased EELI to a similar extent (mean percentage change, 198% [95% CI, 67–330%]; $P = 0.001$; 263% [95% CI, 121 to 407%]; $P = 0.001$, respectively) (Figure 4). The most relevant increase in EELI was observed in dorsal lung regions.

Dynamic lung strain during helmet CPAP and NIV was lower than that during HFNO (mean difference, −0.20 [95% CI, −0.37 to −0.04]; $P = 0.01$; −0.17 [95% CI, −0.32 to −0.02]; $P = 0.05$, respectively), with no difference between CPAP and NIV ($P > 0.99$) (Figure 4). The reduction in dynamic lung strain was associated with a decrease in the percentage of lung regions exhibiting a dynamic strain > 2, which was smaller during CPAP and greater during HFNO (Figure 5).

Table 1. Patients' Demographics

Age, years	66 (62–75)
Sex, female, no. (%)	2 (13)
Height, cm	175 (170–178)
Body mass index, kg/m²	28 (24–30)
SAPS II	31 (29–37)
SOFA at study inclusion	2 (2–2)
COVID-19 as the cause of respiratory failure	10 (67)
Hematological malignancies, no.(%)	3 (20)
Duration of Non-Invasive respiratory support before enrollment, hours	
Non-Invasive Ventilation	0 (0–0)
Continuous Positive Airway Pressure	0 (0–0)
High Flow Nasal Oxygen	0 (0–12)
Bilateral infiltrates at study inclusion	14 (93)
$Pa_{O_2}/F_{I_{O_2}}$ during face mask O_2	120 (103–137)
Pa_{CO_2} during face mask O_2	34 (27–36)
Glasgow Coma Scale score on inclusion	15 (15–15)
Treatment failure after the enrollment – need for endotracheal intubation, no. (%)	4 (27)
Length of ICU stay, days	13 (5–19)
In-ICU mortality no. (%)	6 (40)

Data are reported as medians (Interquartile range), unless specified otherwise.

Table 2. Effort to Breathe, Respiratory Mechanics, Gas Exchange, and Hemodynamics

	HFNO	Helmet CPAP	Helmet NIV	P Value* HFNO vs. CPAP	P Value† HFNO vs. NIV	P Value‡ CPAP vs. NIV
Effort to breathe and respiratory mechanics						
ΔP_{ES}, cm H_2O	10 (8 to 13)	13 (10 to 19)	5 (3 to 9)	0.17	0.01	0.001
Quasi-static ΔP_L, cm H_2O	9 (8 to 10)	12 (7 to 18)	13 (8 to 17)	0.26	0.13	>0.99
PEEP, cm H_2O	2.5§	13.5 (12.1 to 14.8)	13.6 (12.7 to 15.1)	0.001	0.001	>0.99
Respiratory rate, breaths/min	26 (21 to 32)	30 (25 to 34)	28 (23 to 33)	0.29	>0.99	0.15
P_{ES} pressure–time product per minute, cm $H_2O \cdot sec \cdot min^{-1}$	215 (143 to 305)	299 (234 to 437)	181 (88 to 236)	0.34	0.56	0.002
Mean airway expiratory pressure, cm H_2O	2.5§	14 (12 to 15)	16 (16 to 19)	0.001	0.001	0.001
Mean transpulmonary expiratory pressure, cm H_2O	−5 (−13 to −3)	0 (−3 to 3)	−1 (−4 to 5)	0.001	0.001	>0.99
Esophageal pressure, end-expiratory, cm H_2O	7 (6 to 16)	14 (11 to 17)	14 (10 to 18)	0.02	0.03	>0.99
Transpulmonary pressure, mean pressure, cm H_2O	−5 (−13 to −3)	0 (0 to 3 to 3)	1 (−1 to 7)	0.001	0.001	0.13
Inspiratory time, s	1.14 (0.77 to 1.49)	1.01 (0.79 to 1.26)	1.06 (0.84 to 1.29)	>0.99	>0.99	>0.99
Expiratory time, s	1.26 (0.96 to 1.52)	1.08 (0.70 to 1.24)	1.20 (0.96 to 1.37)	0.88	>0.99	0.73
Dyspnea, VAS	3 (0 to 6)	2 (0 to 5)	2 (0 to 4)	0.55	0.21	>0.99
Self-assessed discomfort, VAS	2 (0 to 4)	4 (2 to 6)	4 (1 to 7)	0.008	0.11	>0.99
Gas exchange						
F_{IO_2}	0.6 (0.5 to 0.6)	0.6 (0.5 to 0.6)	0.6 (0.5 to 0.6)	0.23	0.25	>0.99
Pa_{O_2}	67 (60 to 75)	105 (84 to 140)	87 (81 to 110)	0.001	0.001	0.14
Pa_{O_2}/F_{IO_2}	120 (107 to 149)	175 (158 to 281)	166 (136 to 215)	0.001	0.002	0.13
Sp_{O_2}	93 (86 to 95)	97 (94 to 98)	95 (93 to 97)	0.40	0.12	0.025
Sp_{O_2}/F_{IO_2}	158 (142 to 182)	165 (163 to 194)	162 (158 to 188)	0.03	0.07	0.02
Pa_{CO_2}	32 (26 to 35)	34 (27 to 38)	35 (28 to 37)	0.09	0.10	>0.99
Hemodynamics						
Heart rate, beats/min	81 (70 to 91)	79 (70 to 92)	80 (70 to 92)	>0.99	>0.99	>0.99
Arterial pressure, mm Hg						
Systolic	137 (130 to 160)	140 (120 to 163)	141 (124 to 154)	0.65	0.94	>0.99
Mean	87 (80 to 96)	90 (81 to 102)	87 (80 to 98)	0.35	>0.99	>0.99
Diastolic	62 (60 to 70)	68 (60 to 70)	67 (60 to 77)	>0.99	0.33	0.21

Definition of abbreviations: CPAP = continuous positive airway pressure; HFNO = high-flow nasal oxygen; NIV = noninvasive ventilation; PEEP = positive end-expiratory pressure; P_{ES} = esophageal pressure; P_L = transpulmonary pressure; Sp_{O_2} = oxygen saturation as measured by pulse oximetry; VAS = visual analog scale; ΔP_{ES} = inspiratory effort; ΔP_L = transpulmonary pressure.
Data are reported as median (interquartile range). All paired comparisons were adjusted with Bonferroni's or Dunn's correction, as appropriate. *P* values ≤ 0.05 are considered statistically significant.
*Comparison between HFNO and helmet CPAP.
†Comparison between HFNO and helmet NIV.
‡Comparison between helmet CPAP and helmet NIV.
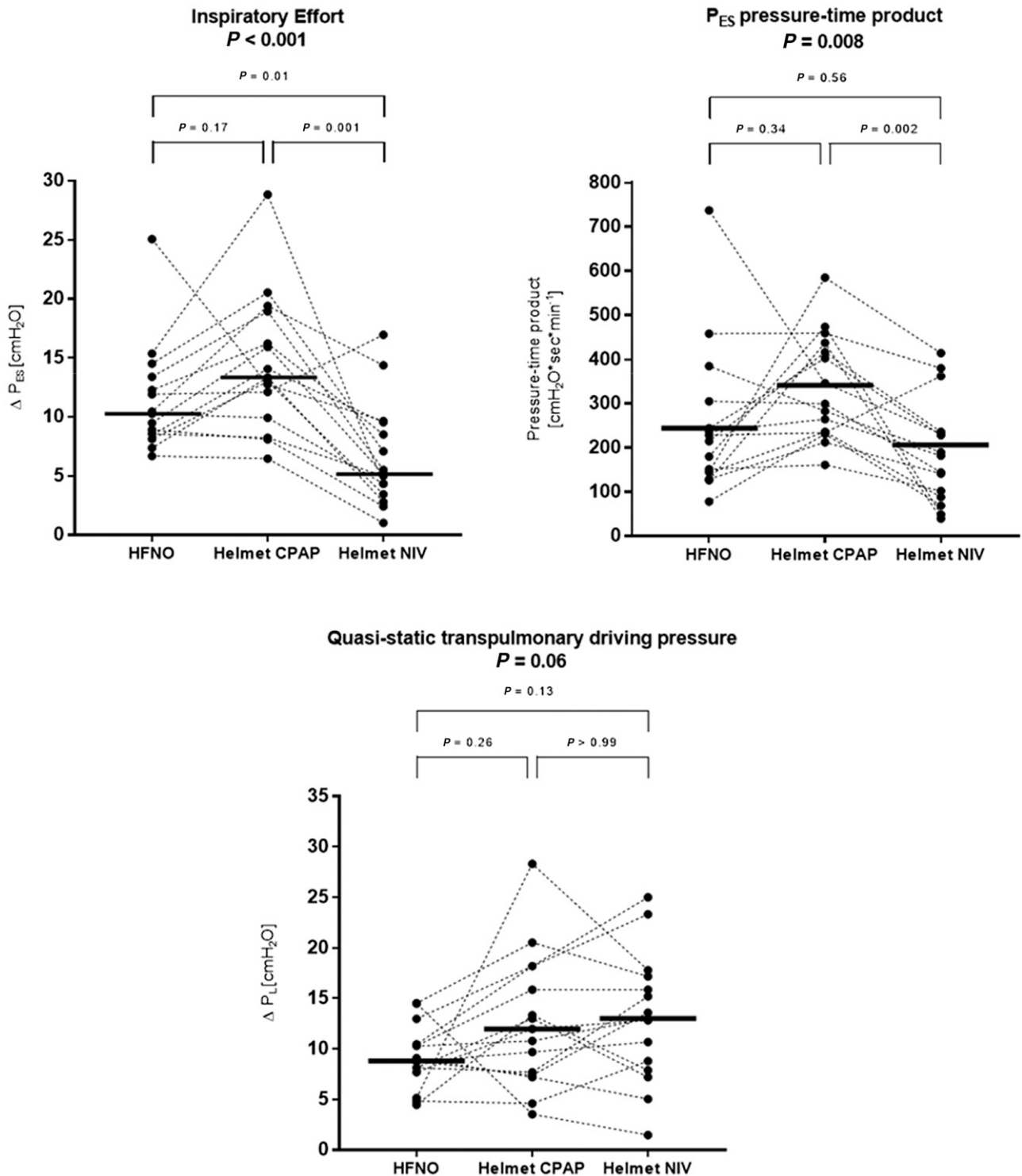§The airway pressure during HFNO was not measured but assumed to be constant at 2.5 cm H_2O.

Figure 2. Individual patient values and medians of inspiratory effort (ΔP_{ES}) swings, pressure–time product of the P_{ES} (PTP_{ES}), and quasistatic transpulmonary pressure (ΔP_L) during the three phases of the study. Compared with high-flow nasal oxygen (HFNO) and helmet continuous positive airway pressure (CPAP), helmet NIV reduced inspiratory effort (ΔP_{ES}) and muscle workload only compared with CPAP (PTP_{ES}). ΔP_L was not different between treatments. NIV = noninvasive ventilation.
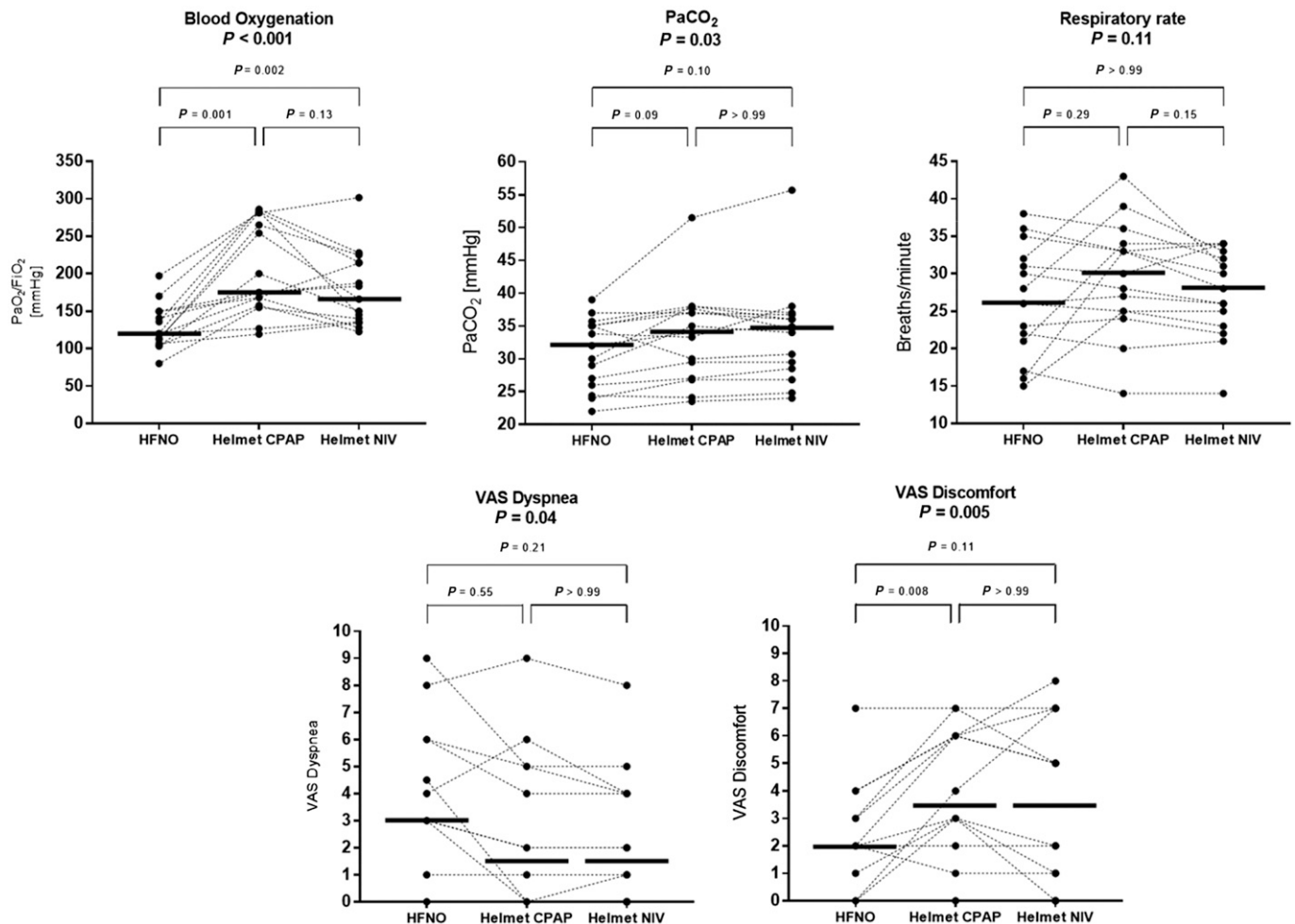
Figure 3. Individual patient values and medians of $Pa_{O_2}/F_{I_{O_2}}$, Pa_{CO_2}, respiratory rate, and visual analog score (VAS)-measured patient dyspnea and discomfort during the three phases of the study. NIV and helmet continuous positive airway pressure (CPAP) yielded higher $Pa_{O_2}/F_{I_{O_2}}$ than HFNO. Pa_{CO_2}, respiratory rate, and VAS dyspnea were not different between treatments. Discomfort increased during CPAP. HFNO = high-flow nasal oxygen; NIV = noninvasive ventilation.

Discussion

To the best of our knowledge, this is the first study providing a comprehensive evaluation of the physiological effects of high-PEEP helmet NIV and CPAP in hypoxemic respiratory failure. Our results showed that, compared with HFNO:

- helmet NIV, but not CPAP, decreases ΔP_{ES}; the benefit of helmet NIV on ΔP_{ES} is prominent in cases in which ΔP_{ES} is high during HFNO and CPAP;
- helmet NIV and CPAP do not affect ΔP_L, although increases in ΔP_L can occur during NIV in patients exhibiting low ΔP_{ES} during HFNO;

- helmet NIV and CPAP similarly improve blood oxygenation without affecting Pa_{CO_2};
- helmet CPAP and NIV similarly increase EELI and V_T, mostly through increased aeration and ventilation of dorsal lung regions;
- despite the increased V_T, dynamic lung strain is reduced to a similar extent by helmet NIV and CPAP;
- the pendelluft phenomenon is common in nonintubated patients. Helmet support reduces pendelluft, especially when applied in the NIV mode.

Helmet noninvasive support can improve the management of hypoxemic respiratory failure (43). In recent years, early

management of acute hypoxemic respiratory failure has focused on obtaining a balance between the oxygenation improvement provided by noninvasive techniques and the need for lung and diaphragm protection when spontaneous breathing is preserved (4, 44–46). The application of high PEEP improves oxygenation, modulates inspiratory effort, and limits ventilatory heterogeneities caused by the pendelluft phenomenon (12, 13). Although achieving high PEEP is difficult with face masks, it is feasible with the helmet interface. In our physiological trial designed to assess the effects of high PEEP with and without pressure support delivered through the helmet interface in patients with acute hypoxemic respiratory failure, we used HFNO as a comparator. High-flow oxygen is the suggested

Table 3. Electrical Impedance Tomography-derived Measures

	HFNO	Helmet CPAP	Helmet NIV	P value* HFNO vs. CPAP	P Value† HFNO vs. NIV	P value‡ CPAP vs. NIV
Tidal impedance variation, arbitrary units§	913 (781–1,294)	1,775 (1,289–2,788)	1,411 (1,047–1,842)	0.002	0.02	0.32
Ventral ROI	53 (33–74)	54 (38–82)	64 (31–95)	>0.99	>0.99	>0.99
Midventral ROI	255 (205–521)	399 (301–667)	374 (184–605)	0.03	>0.99	0.20
Middorsal ROI	455 (343–618)	944 (680–1,062)	770 (468–910)	0.001	0.03	0.17
Dorsal ROI	163 (124–181)	325 (260–427)	254 (171–368)	0.001	0.02	0.51
Quasistatic lung compliance, arbitrary units/cm H_2O§	132 (64–143)	153 (84–239)	121 (77–190)	0.16	>0.99	>0.99
Quasistatic ventral ROI compliance	5 (3–10)	5 (3–8)	5 (4–9)	>0.99	>0.99	>0.99
Quasistatic midventral ROI compliance	34 (17–51)	37 (21–68)	29 (19–70)	0.82	>0.99	>0.99
Quasistatic middorsal ROI compliance	56 (35–72)	90 (42–115)	61 (33–107)	0.10	0.96	>0.99
Quasistatic dorsal ROI compliance	17 (10–28)	27 (16–36)	19 (12–32)	0.10	0.98	>0.99
Pendelluft effect, % of tidal impedance variation	55 (25–68)	31 (11–44)	26 (8–44)	0.01	0.004	0.16
Estimated EELI, arbitrary units	1,809 (873–1,964)	5,028 (3,051–6,738)	4,301 (2,363–6,358)	0.001	0.001	0.47
Estimated EELI, ventral ROI	45 (17–61)	141 (69–229)	95 (70–207)	0.001	0.001	>0.99
Estimated EELI, midventral ROI	509 (317–649)	1,490 (948–2,242)	1,161 (686–2,021)	0.001	0.001	0.29
Estimated EELI, middorsal ROI	908 (522–1,037)	2,707 (1,739–3,396)	2,103 (1,201–3,273)	0.001	0.001	>0.99
Estimated EELI, dorsal ROI	221 (154–328)	712 (523–898)	581 (332–847)	0.001	0.001	0.17
Dynamic lung strain	0.64 (0.56–0.76)	0.41 (0.29–0.66)	0.50 (0.31–0.67)	0.01	0.05	>0.99
Regional dynamic strain, ventral ROI	1.14 (0.93–1.8)	1.54 (0.95–2.5)	1.79 (0.81–3.06)	0.30	0.24	0.52
Regional dynamic strain, midventral ROI	0.60 (0.55–0.89)	0.97 (0.70–1.49)	0.96 (0.48–1.38)	0.06	0.25	0.99
Regional dynamic strain, middorsal ROI	0.62 (0.43–0.77)	0.33 (0.20–0.52)	0.37 (0.23–0.57)	0.007	0.16	0.68
Regional dynamic strain, dorsal ROI	0.67 (0.57–0.96)	0.43 (0.23–0.64)	0.49 (0.28–0.60)	0.03	0.01	>0.99
Overstretched pixels,‖ global, %	4 (3–9)	1 (1–3)	2 (1–3)	0.02	0.40	0.50
Overstretched pixels, ventral ROI, %	20 (16–27)	9 (6–16)	10 (4–17)	0.006	0.07	>0.99
Overstretched pixels, midventral ROI, %	3 (1–9)	1 (0–2)	1 (0–3)	0.23	>0.99	0.11
Overstretched pixels, middorsal ROI, %	1 (0–7)	0 (0–1)	0 (0–0)	0.09	0.21	>0.99
Overstretched pixels, dorsal ROI, %	3 (1–9)	0 (0–1)	0 (0–1)	0.01	0.49	0.64

Definition of abbreviations: CPAP = continuous positive airway pressure; EELI = end-expiratory lung impedance; HFNO = high-flow nasal oxygen; NIV = noninvasive ventilation; ROI = region of interest.

Data are reported as the median (interquartile range). All paired comparisons were adjusted with Bonferroni's or Dunn's correction, as appropriate. *P* values ≤ 0.05 are considered statistically significant.

*Comparison between HFNO and helmet CPAP.
†Comparison between HFNO and helmet NIV.
‡Comparison between helmet CPAP and helmet NIV.
§All calculations are based on pixel-by-pixel analysis of the electrical impedance tomography signal. V_T and compliance calculated as the absolute difference between end-inspiratory and end-expiratory lung impedance, which does not take into account the regional inflation/deflation due to pendelluft, is displayed in Table E1.
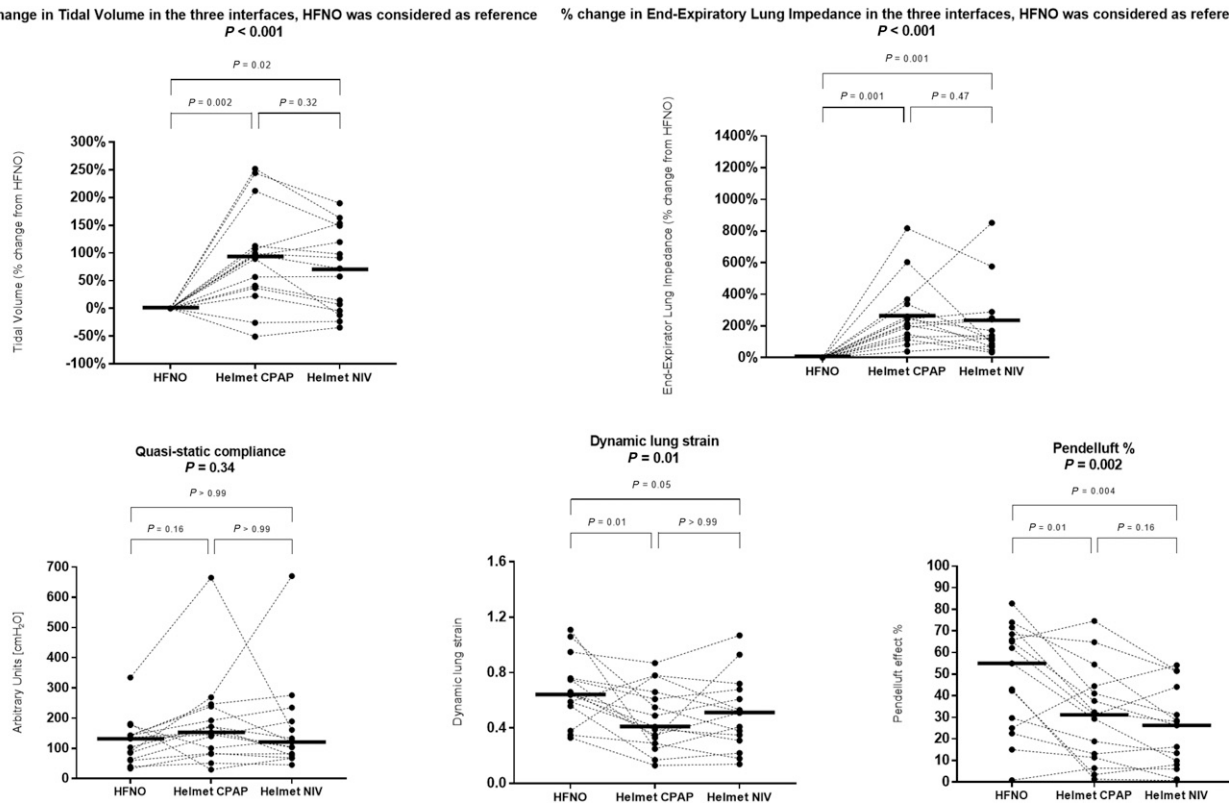‖Overstretched pixels are defined as those with a dynamic strain >2.

Figure 4. Individual patient values and medians of the impedance-derived measures during high-flow nasal oxygen (HFNO), helmet continuous positive airway pressure (CPAP), and helmet noninvasive ventilation (NIV). Both helmet NIV and helmet CPAP increased the V_T compared with HFNO. Quasistatic respiratory system compliance was similar between HFNO and helmet NIV and showed a trend toward an increase during helmet CPAP. The application of positive end-expiratory pressure caused a significant increase in the end-expiratory lung impedance, which was related to recruitment in the dorsal lung regions, so the dynamic lung strain during helmet NIV and helmet CPAP decreased. Because of increased aeration of the dependent lung regions, both helmet NIV and helmet CPAP reduced the pendelluft effect.

intervention for noninvasive management of acute hypoxemic respiratory failure and is the most widely used device to treat these patients (1).

Effort to Breathe and Respiratory Mechanics

Helmet NIV, but not CPAP, decreased ΔP_{ES} compared with HFNO, likely as an effect of pressure support (42). In intubated patients with hypoxemic respiratory failure, high PEEP decreases ΔP_{ES} (12) through electromechanical uncoupling of the diaphragm. Conversely, in our study, high PEEP alone delivered through the helmet did not produce the same effect. In our study, the use of high PEEP was combined with a change in the interface for delivering support. Although HFNO produces airway dead space washout, the helmet has a large internal volume that generates some CO_2 rebreathing. Our data indicate that when high PEEP is applied in the CPAP mode,

ΔP_{ES} may be equal to, or even greater than, that during HFNO. Conversely, helmet NIV enables the greatest reduction in ΔP_{ES} because of pressure support. The different effects on ΔP_{ES} are the major physiological difference between helmet CPAP and NIV.

Importantly, patients with hypocapnia had the most intense ΔP_{ES} while on CPAP and HFNO. These patients had the greatest reduction in ΔP_{ES} during NIV and may possibly represent a subphenotype that can clinically benefit the most from helmet NIV (47). Conversely, in patients with low ΔP_{ES} during HFNO, CPAP may be sufficient to improve oxygenation, and helmet NIV may not be needed or even contraindicated because it can increase ΔP_L. Accordingly, ΔP_L was lowest during HFNO and highest during NIV. Although the difference was not significant, consistent with the previous considerations of ΔP_{ES}, patients exhibiting low inspiratory effort while on HFNO developed increases

in ΔP_L during helmet NIV. This condition may be particularly common among patients with COVID-19, who have average lower inspiratory effort compared with respiratory failure from other causes (48, 49).

During controlled mechanical ventilation, limiting ΔP_L and tidal volume is mandatory to reduce ventilator-induced lung injury. Conversely, during spontaneous breathing, this does not necessarily provide lung protection because of the possible occurrence of ventilatory inhomogeneities (such as the pendelluft phenomenon) and high regional stress due to heterogeneous transmission of intense ΔP_{ES} (44, 50). It is unknown whether the slight increase in ΔP_L produced by helmet NIV (4 cm H_2O, on average), which mostly pertains to patients with low ΔP_{ES} during HFNO, may be injurious, especially if helmet NIV is associated with a significant ΔP_{ES} reduction, as in our study. In addition, ΔP_L during helmet NIV may have been overestimated in
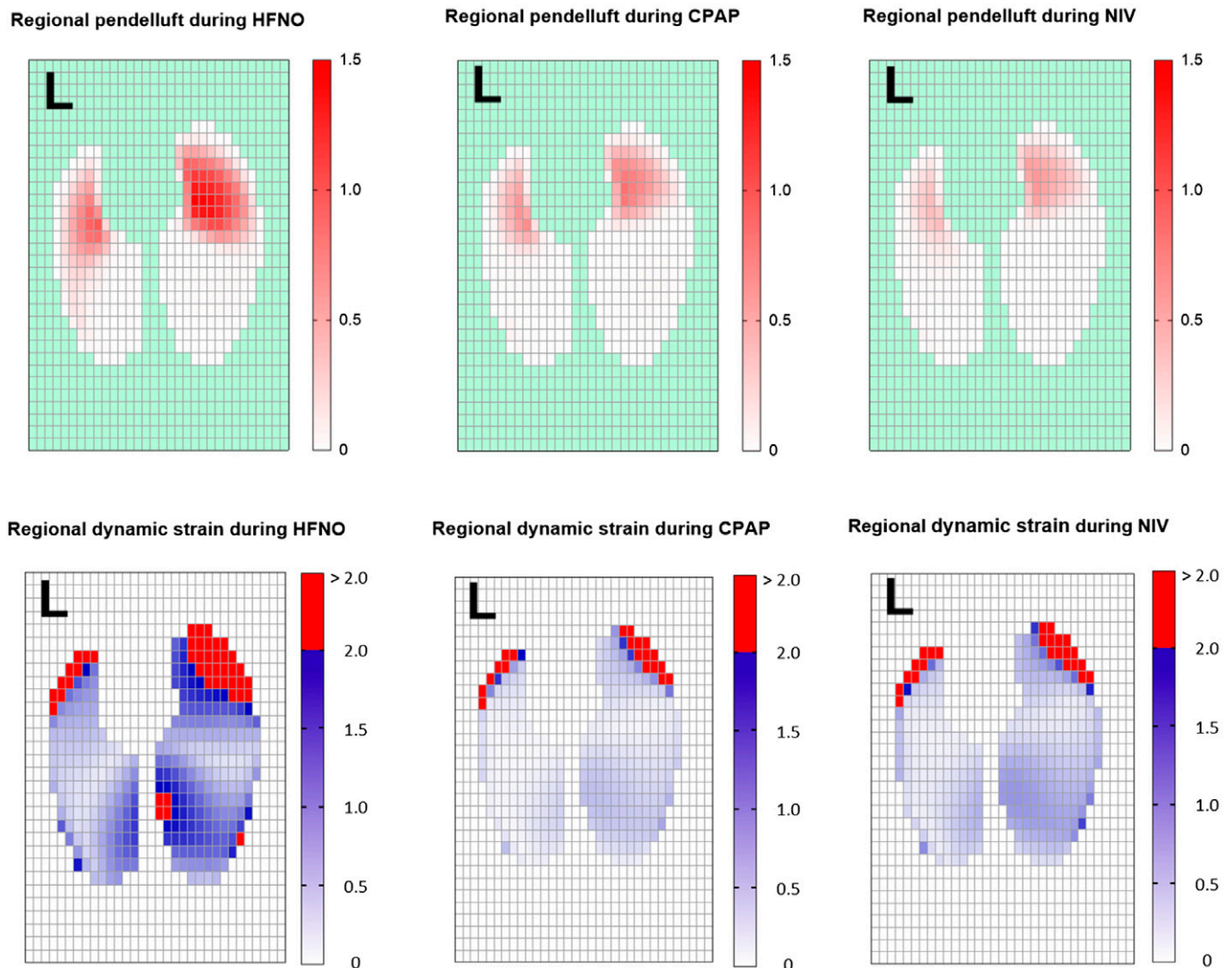
Figure 5. Intrapulmonary distribution of air in one representative patient. The patient showed a high pendelluft percentage during HFNO (65% of VT), which progressively decreased with both helmet CPAP (38% of VT) and NIV (26% of VT) (top): red pixels represent those deflating during inspiration, with color intensity displaying percentage of VT contributing to pendelluft. Consistent with the reduction in pendelluft and the increase in end-expiratory lung impedance, there was a reduction in the global and regional dynamic strain (bottom row). In addition, there was a reduction in the amounts of the regions where dynamic strain was >2 (in red in the bottom row). CPAP = continuous positive airway pressure; HFNO = high-flow nasal oxygen; NIV = noninvasive ventilation.

our study because part of the pressure support was dissipated to distend the interface. This could justify, at least in part, the increase in ΔP_L observed during NIV (23).

Our study showed no significant difference in respiratory rate among the three interfaces. This finding, although different from that of a previous report comparing HFNO and helmet NIV in patients with hypoxemia without COVID-19 (42), is consistent with a recent randomized trial showing similar respiratory rates in patients with COVID-19 respiratory failure treated with helmet NIV or HFNO (15). It is reasonable that the inclusion of patients with COVID-19, who less often show a dysregulated respiratory drive (49), contributed to these results.

Gas Exchange and Interface Tolerance

In our study, both helmet CPAP and NIV increased Pa_{O_2}/Fi_{O_2}, likely because of PEEP-induced recruitment of dorsal lung regions (51). CPAP and NIV showed a trend toward increased Pa_{CO_2} despite higher VT and $\dot{V}_E$. Although HFNO provides anatomical dead space clearance, facilitating CO_2 washout (27, 52, 53), the helmet interface increases dead space and causes CO_2 rebreathing even when the flow of fresh gas entering the system is adequate (24). However, in our study, Pa_{CO_2} remained within the physiological range in all but one patient during helmet support.

In our cohort, the helmet was less well tolerated than HFNO, especially when applied in the CPAP mode. Recently, dexmedetomidine has been shown to

improve tolerance to NIV (54) and aid patients experiencing discomfort while undergoing helmet support.

EELI, V_T Size, and Distribution

Helmet CPAP and helmet NIV resulted in similar increases in EELI through improved aeration of dorsal lung regions, which is consistent with the physiological mechanism of PEEP in patients with acute hypoxemic respiratory failure and acute respiratory distress syndrome (51, 55).

Compared with HFNO, helmet CPAP and helmet NIV increased V_T. This resulted from the combination of small increases in ΔP_L and compliance. The increase in ΔP_L was due to a slightly higher ΔP_{ES} during CPAP and to the presence of pressure support with reduced ΔP_{ES} during NIV. Notably, most of the increase in V_T occurred in dorsal regions, suggesting ventilation of previously collapsed lung tissue.

Although V_T increased with both helmet CPAP and NIV, lung dynamic strain was reduced compared with HFNO. Dynamic strain is the mechanical distortion produced by V_T in the aerated lung and is among the key mechanisms of ventilator-induced lung injury. Dynamic strain is particularly harmful when the inflated volume is two times larger than the functional residual capacity (35, 38, 39, 56). In our study, the percentage of overstretched lung areas (i.e., those with a dynamic strain > 2) was higher during HFNO and lower during CPAP. This is an effect of PEEP that promotes the distribution of V_T toward the dorsal-dependent lung regions.

Pendelluft is an intratidal shift of gas from nondependent to dependent lung regions. Pendelluft occurs at the beginning of inspiration and generates local overstretching and progression of lung injury in the dependent lung (36, 57). We detected pendelluft involving $>10\%$ of V_T in 14/15 patients in our study. This high prevalence was probably due to the high sensitivity of our system, which included pixel-by-pixel assessment of the electrical impedance tomography signal. Pendelluft implies the presence of atelectatic lung regions and a vertical gradient in ΔP_{ES}. This is consistent with the fact that, in our study, the amount of pendelluft was higher among patients with low $Pa_{O_2}/F_{I_{O_2}}$ (i.e., those with a higher lung weight) and intense ΔP_{ES} (58). The occurrence of pendelluft can be mitigated by reducing inspiratory effort and

applying PEEP (13). Accordingly, both helmet CPAP (application of PEEP) and helmet NIV (application of PEEP combined with ΔP_{ES} reduction) reduced pendelluft compared with HFNO, with NIV being the most effective intervention.

Clinical Implications

In clinical practice, helmet CPAP and NIV are applied interchangeably (12). However, our study demonstrates that their mechanisms of action are profoundly different. Although both techniques improve hypoxemia and limit pendelluft, NIV also reduces ΔP_{ES} and respiratory muscle workload, which is not the case for CPAP. Helmet NIV may result in increases in ΔP_L, especially in patients who have low inspiratory effort before treatment start or during HFNO. These physiological findings suggest that treatment individualization may be considered in patients with hypoxemia who are eligible for helmet support. When ΔP_{ES} before treatment start or during HFNO is low, HFNO may be preferable; helmet CPAP may represent a strategy to improve oxygenation and alveolar recruitment and to partially limit pendelluft. Conversely, when ΔP_{ES} before treatment start or during HFNO is high, helmet NIV may be the best choice. If ΔP_{ES} monitoring is unavailable, hypocapnia, in the absence of metabolic alterations, could help estimate intense ΔP_{ES} and identify patients who may most benefit from helmet NIV (47). When available, ΔP_{ES} should be strictly monitored, as the lack of ΔP_{ES} reduction soon after NIV start represents an early predictor of treatment failure (48).

Helmet CPAP and NIV increased V_T to a similar extent. The harmful effects of high V_T during spontaneous breathing are well described (59). However, with helmet CPAP and NIV, the PEEP-induced increase in aeration of dorsal regions reduced dynamic lung strain and pendelluft. Future studies will be needed to establish the best targets for safe spontaneous breathing in patients with hypoxemia among ΔP_{ES}, ΔP_L, V_T, pendelluft, and dynamic strain.

Limitations

First, calculation of EELI is an indirect measure that relies on the relationship between lung stress and strain; absolute values should be interpreted cautiously. Second, our calculations of strain assume that all PEEP-induced aeration increases in

dorsal regions are due to recruitment; albeit physiologically sound, this is an approximation (40). Third, to calculate the P_{ES} pressure–time product, we partitioned respiratory system mechanics assuming a constant ratio between chest wall and respiratory system elastance; unfortunately, measurement of chest wall compliance is not otherwise possible in nonintubated patients (34). Fourth, the nasogastric tube used for esophageal manometry may have interfered with flow delivery during HFNO. However, this limitation is similar to that of other previous investigations showing HFNO benefits in terms of ΔP_{ES} reduction and increases in EELI (27, 60). Fifth, to compute transpulmonary pressure at end-expiration, airway pressure during HFNO was assumed to be constant and equal to 2.5 cm H_2O (27); however, this did not affect the calculations of ΔP_{ES} and ΔP_L, which represent the most relevant results of our study. Sixth, the correct positioning of the esophageal balloon was not validated with the occlusion test; thus, the esophageal and transpulmonary pressure values should be interpreted with caution. Finally, we did not measure transdiaphragmatic pressure; hence, we could not determine whether expiratory muscle activity may have affected our results.

Conclusions

Compared with HFNO in patients with hypoxemic respiratory failure, helmet NIV, but not CPAP, reduces ΔP_{ES}. ΔP_L is not significantly different between treatments, but patients who exhibit low ΔP_{ES} while on HFNO may develop increases in ΔP_L during NIV. Helmet CPAP and NIV improve oxygenation to a similar extent, mostly because of the PEEP-induced increase in aeration in dorsal lung regions. Both NIV and CPAP increase V_T but significantly reduce dynamic lung strain. Helmet NIV and, to a lesser extent, helmet CPAP mitigate the occurrence of pendelluft. ∎

References

1. Oczkowski S, Ergan B, Bos L, Chatwin M, Ferrer M, Gregoretti C, *et al.* ERS clinical practice guidelines: high-flow nasal cannula in acute respiratory failure. *Eur Respir J* 2022;59:2101574.
2. Ranieri VM, Tonetti T, Navalesi P, Nava S, Antonelli M, Pesenti A, *et al.* High-flow nasal oxygen for severe hypoxemia: oxygenation response and outcome in patients with COVID-19. *Am J Respir Crit Care Med* 2022;205:431–439.
3. Ferreyro BL, Angriman F, Munshi L, Del Sorbo L, Ferguson ND, Rochwerg B, *et al.* Association of noninvasive oxygenation strategies with all-cause mortality in adults with acute hypoxemic respiratory failure: a systematic review and meta-analysis. *JAMA* 2020;324:57–67.
4. Brochard L, Slutsky A, Pesenti A. Mechanical ventilation to minimize progression of lung injury in acute respiratory failure. *Am J Respir Crit Care Med* 2017;195:438–442.
5. Menga LS, Berardi C, Ruggiero E, Grieco DL, Antonelli M. Noninvasive respiratory support for acute respiratory failure due to COVID-19. *Curr Opin Crit Care* 2022;28:25–50.
6. Rittayamai N, Grieco DL, Brochard L. Noninvasive respiratory support in intensive care medicine. *Intensive Care Med* 2022;48:1211–1214.
7. Grieco DL, Patel BK, Antonelli M. Helmet noninvasive support in hypoxemic respiratory failure. *Intensive Care Med* 2022;48:1072–1075.
8. Antonelli M, Conti G, Pelosi P, Gregoretti C, Pennisi MA, Costa R, *et al.* New treatment of acute hypoxemic respiratory failure: noninvasive pressure support ventilation delivered by helmet—a pilot controlled trial. *Crit Care Med* 2002;30:602–608.
9. Briel M, Meade M, Mercat A, Brower RG, Talmor D, Walter SD, *et al.* Higher vs lower positive end-expiratory pressure in patients with acute lung injury and acute respiratory distress syndrome: systematic review and meta-analysis. *JAMA* 2010;303:865–873.
10. Cesarano M, Grieco DL, Michi T, Munshi L, Menga LS, Delle Cese L, *et al.* Helmet noninvasive support for acute hypoxemic respiratory failure: rationale, mechanism of action and bedside application. *Ann Intensive Care* 2022;12:94.
11. Yoshida T, Roldan R, Beraldo MA, Torsani V, Gomes S, De Santis RR, *et al.* Spontaneous effort during mechanical ventilation: maximal injury with less positive end-expiratory pressure. *Crit Care Med* 2016;44: e678–e688.
12. Morais CCA, Koyama Y, Yoshida T, Plens GM, Gomes S, Lima CAS, *et al.* High positive end-expiratory pressure renders spontaneous effort noninjurious. *Am J Respir Crit Care Med* 2018;197:1285–1296.
13. Yoshida T, Grieco DL, Brochard L, Fujino Y. Patient self-inflicted lung injury and positive end-expiratory pressure for safe spontaneous breathing. *Curr Opin Crit Care* 2020;26:59–65.
14. Patel BK, Wolfe KS, Pohlman AS, Hall JB, Kress JP. Effect of noninvasive ventilation delivered by helmet vs face mask on the rate of endotracheal intubation in patients with acute respiratory distress syndrome: a randomized clinical trial. *JAMA* 2016;315:2435–2441.
15. Grieco DL, Menga LS, Cesarano M, Rosà T, Spadaro S, Bitondo MM, *et al.*; COVID-ICU Gemelli Study Group. Effect of helmet noninvasive ventilation vs high-flow nasal oxygen on days free of respiratory support in patients with COVID-19 and moderate to severe hypoxemic respiratory failure: the HENIVOT randomized clinical trial. *JAMA* 2021; 325:1731–1743.
16. Arabi YM, Aldekhyl S, Al Qahtani S, Al-Dorzi HM, Abdukahil SA, Al Harbi MK, *et al.*; Saudi Critical Care Trials Group. Effect of helmet noninvasive ventilation vs usual respiratory support on mortality among patients with acute hypoxemic respiratory failure due to COVID-19: the HELMET-COVID randomized clinical trial. *JAMA* 2022;328:1063–1072.
17. Menga LS, Cese LD, Bongiovanni F, Lombardi G, Michi T, Luciani F, *et al.* High failure rate of noninvasive oxygenation strategies in critically ill subjects with acute hypoxemic respiratory failure due to COVID-19. *Respir Care* 2021;66:705–714.
18. Menga LS, delle Cese L, Rosà T, Cesarano M, Michi T, Grieco DL, *et al.* EIT findings during helmet noninvasive support [abstract]; 2022 [accessed 2022 Aug 21]. Available from: https://www.plugwgroup.org/_files/ugd/ 28da57_a3648f16b8654961b699c819d5456d91.pdf.
19. Frat J-P, Thille AW, Mercat A, Girault C, Ragot S, Perbet S, *et al.*; FLORALI Study Group; REVA Network. High-flow oxygen through nasal cannula in acute hypoxemic respiratory failure. *N Engl J Med* 2015;372:2185–2196.
20. Grieco DL, Toni F, Santantonio MT, Spaziani L, Natalini D, Idone FA, *et al.* Comfort during high-flow oxygen therapy through nasal cannula in critically ill patients: effects of gas temperature and flow. *Intensive Care Med* 2013;39:512.
21. Bongiovanni F, Grieco DL, Anzellotti GM, Menga LS, Michi T, Cesarano M, *et al.* Gas conditioning during helmet noninvasive ventilation: effect on comfort, gas exchange, inspiratory effort, transpulmonary pressure and patient-ventilator interaction. *Ann Intensive Care* 2021;11:184.
22. Mojoli F, Iotti GA, Currò I, Pozzi M, Via G, Venti A, *et al.* An optimized set-up for helmet noninvasive ventilation improves pressure support delivery and patient-ventilator interaction. *Intensive Care Med* 2013;39: 38–44.
23. Vargas F, Thille A, Lyazidi A, Campo FR, Brochard L. Helmet with specific settings versus facemask for noninvasive ventilation. *Crit Care Med* 2009;37:1921–1928.
24. Taccone P, Hess D, Caironi P, Bigatello LM. Continuous positive airway pressure delivered with a "helmet": effects on carbon dioxide rebreathing. *Crit Care Med* 2004;32:2090–2096.
25. Mojoli F, Chiumello D, Pozzi M, Algieri I, Bianzina S, Luoni S, *et al.* Esophageal pressure measurements under different conditions of intrathoracic pressure: an in vitro study of second generation balloon catheters. *Minerva Anestesiol* 2015;81:855–864.
26. Mauri T, Yoshida T, Bellani G, Goligher EC, Carteaux G, Rittayamai N, *et al.*; PLeUral pressure working Group (PLUG—Acute Respiratory Failure section of the European Society of Intensive Care Medicine). Esophageal and transpulmonary pressure in the clinical setting: meaning, usefulness and perspectives. *Intensive Care Med* 2016;42: 1360–1373.
27. Mauri T, Turrini C, Eronia N, Grasselli G, Volta CA, Bellani G, *et al.* Physiologic effects of high-flow nasal cannula in acute hypoxemic respiratory failure. *Am J Respir Crit Care Med* 2017;195:1207–1215.
28. Frerichs I, Amato MBP, van Kaam AH, Tingay DG, Zhao Z, Grychtol B, *et al.*; TREND study group. Chest electrical impedance tomography examination, data analysis, terminology, clinical use and recommendations: consensus statement of the TRanslational EIT developmeNt stuDy group. *Thorax* 2017;72:83–93.
29. ATS Committee on Proficiency Standards for Clinical Pulmonary Function Laboratories. ATS statement: guidelines for the six-minute walk test. *Am J Respir Crit Care Med* 2002;166:111–117.
30. Puntillo KA, Morris AB, Thompson CL, Stanik-Hutt J, White CA, Wild LR. Pain behaviors observed during six common procedures: results from Thunder Project II. *Crit Care Med* 2004;32:421–427.
31. Menga LS, Grieco DL, Rosà T, Cesarano M, Delle Cese L, Berardi C, *et al.* Dyspnoea and clinical outcome in critically ill patients receiving noninvasive support for COVID-19 respiratory failure: *post hoc* analysis of a randomised clinical trial. *ERJ Open Res* 2021;7:00418-2021.
32. Dres M, Similowski T, Goligher EC, Pham T, Sergenyuk L, Telias I, *et al.* Dyspnoea and respiratory muscle ultrasound to predict extubation failure. *Eur Respir J* 2021;58:2100334.
33. Sang L, Zhao Z, Yun P-J, Frerichs I, Möller K, Fu F, *et al.* Qualitative and quantitative assessment of pendelluft: a simple method based on electrical impedance tomography. *Ann Transl Med* 2020;8:1216.
34. Chen L, Grieco DL, Beloncle F, Chen G-Q, Tiribelli N, Madotto F, *et al.* Partition of respiratory mechanics in patients with acute respiratory distress syndrome and association with outcome: a multicentre clinical study. *Intensive Care Med* 2022;48:888–898.
35. Protti A, Andreis DT, Monti M, Santini A, Sparacino CC, Langer T, *et al.* Lung stress and strain during mechanical ventilation: any difference between statics and dynamics? *Crit Care Med* 2013;41:1046–1055.
36. Yoshida T, Torsani V, Gomes S, De Santis RR, Beraldo MA, Costa EL, *et al.* Spontaneous effort causes occult pendelluft during mechanical ventilation. *Am J Respir Crit Care Med* 2013;188:1420–1427.
37. Chi Y, Zhao Z, Frerichs I, Long Y, He H. Prevalence and prognosis of respiratory pendelluft phenomenon in mechanically ventilated ICU patients with acute respiratory failure: a retrospective cohort study. *Ann Intensive Care* 2022;12:22.
38. Chiumello D, Carlesso E, Cadringher P, Caironi P, Valenza F, Polli F, *et al.* Lung stress and strain during mechanical ventilation for acute respiratory distress syndrome. *Am J Respir Crit Care Med* 2008;178: 346–355.

39. Protti A, Cressoni M, Santini A, Langer T, Mietto C, Febres D, *et al.* Lung stress and strain during mechanical ventilation: any safe threshold? *Am J Respir Crit Care Med* 2011;183:1354–1362.

40. Protti A, Santini A, Pennati F, Chiurazzi C, Cressoni M, Ferrari M, *et al.* Lung response to a higher positive end-expiratory pressure in mechanically ventilated patients with COVID-19. *Chest* 2022;161: 979–988.

41. Natalini D, Grieco DL, Santantonio MT, Mincione L, Toni F, Anzellotti GM, *et al.* Physiological effects of high-flow oxygen in tracheostomized patients. *Ann Intensive Care* 2019;9:114.

42. Grieco DL, Menga LS, Raggi V, Bongiovanni F, Anzellotti GM, Tanzarella ES, *et al.* Physiological comparison of high-flow nasal cannula and helmet noninvasive ventilation in acute hypoxemic respiratory failure. *Am J Respir Crit Care Med* 2020;201:303–312.

43. Grieco DL, Maggiore SM, Roca O, Spinelli E, Patel BK, Thille AW, *et al.* Non-invasive ventilatory support and high-flow nasal oxygen as first-line treatment of acute hypoxemic respiratory failure and ARDS. *Intensive Care Med* 2021;47:851–866.

44. Yoshida T, Fujino Y, Amato MBP, Kavanagh BP. Fifty years of research in ARDS: spontaneous breathing during mechanical ventilation. Risks, mechanisms, and management. *Am J Respir Crit Care Med* 2017;195: 985–992.

45. Goligher EC, Dres M, Patel BK, Sahetya SK, Beitler JR, Telias I, *et al.* Lung- and diaphragm-protective ventilation. *Am J Respir Crit Care Med* 2020;202:950–961.

46. Grieco DL, Menga LS, Eleuteri D, Antonelli M. Patient self-inflicted lung injury: implications for acute hypoxemic respiratory failure and ARDS patients on non-invasive support. *Minerva Anestesiol* 2019;85: 1014–1023.

47. Grieco DL, Menga LS, Cesarano M, Spadaro S, Bitondo MM, Berardi C, *et al.*; COVID-ICU Gemelli Study Group. Phenotypes of patients with COVID-19 who have a positive clinical response to helmet noninvasive ventilation. *Am J Respir Crit Care Med* 2022; 205:360–364.

48. Tonelli R, Fantini R, Tabbì L, Castaniere I, Pisani L, Pellegrino MR, *et al.* Early inspiratory effort assessment by esophageal manometry predicts noninvasive ventilation outcome in de novo respiratory failure: a pilot study. *Am J Respir Crit Care Med* 2020;202:558–567.

49. Tonelli R, Busani S, Tabbì L, Fantini R, Castaniere I, Biagioni E, *et al.* Inspiratory effort and lung mechanics in spontaneously breathing

50. Yoshida T, Nakahashi S, Nakamura MAM, Koyama Y, Roldan R, Torsani V, *et al.* Volume-controlled ventilation does not prevent injurious inflation during spontaneous effort. *Am J Respir Crit Care Med* 2017;196:590–601.

51. Chen L, Del Sorbo L, Grieco DL, Junhasavasdikul D, Rittayamai N, Soliman I, *et al.* Potential for lung recruitment estimated by the recruitment-to-inflation ratio in acute respiratory distress syndrome: a clinical trial. *Am J Respir Crit Care Med* 2020;201:178–187.

52. Möller W, Celik G, Feng S, Bartenstein P, Meyer G, Oliver E, *et al.* Nasal high flow clears anatomical dead space in upper airway models. *J Appl Physiol (1985)* 2015;118:1525–1532.

53. Pennisi MA, Bello G, Congedo MT, Montini L, Nachira D, Ferretti GM, *et al.* Early nasal high-flow versus Venturi mask oxygen therapy after lung resection: a randomized trial. *Crit Care* 2019;23:68.

54. Belleville JP, Ward DS, Bloor BC, Maze M. Effects of intravenous dexmedetomidine in humans. I. Sedation, ventilation, and metabolic rate. *Anesthesiology* 1992;77:1125–1133.

55. Mauri T, Spinelli E, Scotti E, Colussi G, Basile MC, Crotti S, *et al.* Potential for lung recruitment and ventilation-perfusion mismatch in patients with the acute respiratory distress syndrome from coronavirus disease 2019. *Crit Care Med* 2020;48:1129–1134.

56. Grieco DL, Russo A, Romanò B, Anzellotti GM, Ciocchetti P, Torrini F, *et al.* Lung volumes, respiratory mechanics and dynamic strain during general anaesthesia. *Br J Anaesth* 2018;121:1156–1165.

57. Enokidani Y, Uchiyama A, Yoshida T, Abe R, Yamashita T, Koyama Y, *et al.* Effects of ventilatory settings on pendelluft phenomenon during mechanical ventilation. *Respir Care* 2021;66:1–10.

58. Grieco DL, Menga LS, Conti G, Maggiore SM, Antonelli M. Reply to Spinelli and Mauri: lung and diaphragm protection during noninvasive respiratory support. *Am J Respir Crit Care Med* 2020;201:876–878.

59. Carteaux G, Millán-Guilarte T, De Prost N, Razazi K, Abid S, Thille AW, *et al.* Failure of noninvasive ventilation for de novo acute hypoxemic respiratory failure: role of tidal volume. *Crit Care Med* 2016;44: 282–290.

60. Mauri T, Alban L, Turrini C, Cambiaghi B, Carlesso E, Taccone P, *et al.* Optimum support by high-flow nasal cannula in acute hypoxemic respiratory failure: effects of increasing flow rates. *Intensive Care Med* 2017;43:1453–1463.